Optimization of impulsive discrete-time tumor chemotherapy

Dániel András Drexler
Physiological Controls Research Center
Óbuda University
Budapest, Hungary
drexler.daniel@nik.uni-obuda.hu

Levente Kovács
Physiological Controls Research Center
Óbuda University
Budapest, Hungary
kovacs.levente@nik.uni-obuda.hu

***Abstract*—Cancer therapies, like chemotherapy are generally based on heuristic approaches and expert knowledge. Introducing mathematical and engineering methods into the therapy design process has great potentials in therapy optimization. We investigate the application of a discrete time, impulsive therapy generation algorithm for a model that describes living tumor and dead tumor volume dynamics, drug level dynamics, using mixed-order pharmacokinetics and input saturation. We propose an algorithm that calculates low doses of injections that are required to reach or approximate the best results that can be achieved by the application of the drug. The algorithm is tested based on virtual patients (mice) whose parameters are identified based on measurement from experiments with pegylated liposomal doxorubicin as cytotoxic agent and breast cancer as tumor. The algorithm tested in silico shows much better performance than the protocol used in the experiments.**

***Index Terms*—breast tumor, binary search, cancer treatment**

I. Introduction

In medical practice, treatment of tumor is designed mostly based on expert knowledge using heuristic methods, see e.g., [1]. Model-based personalized treatment is a promising future direction of therapy design that combines mathematical, engineering and physiological knowledge. Model-based therapy design has the potential to provide the optimal therapy, the limitations of this approach are constrained only by the accuracy of the underlying model.

The engineering knowledge is applied to physiological control problems usually by considering continuous time systems and applying discrete time approximation of continuous time controllers. The most common applications, like artificial pancreas [2]–[5], or BIS control in anesthesia [6]–[8], allow the application of this approach, since the control signals (i.e., drug injections) can be delivered with a relatively low sampling time (measured in seconds), allowing efficient discrete time approximations. In most of the papers dealing with tumor therapies, the control problem was considered a continuous time problem as well [9]–[13]. However, the time between the tumor treatments is usually much larger (it is measured in days, compared to the previous examples where the time between the treatments is typically measured in seconds), moreover, the control signals are injections, thus the practical tumor treatment problem is a discrete time impulsive control problem.

This project has received funding from the European Research Council (ERC) under the European Union's Horizon 2020 research and innovation programme (grant agreement No 679681).

Impulsive therapy design for antiangiogenic tumor treatment has been considered as an open-loop model predictive control problem in [14] where the minimal required dose to achieve the specified tumor volume trajectory was calculated using binary search algorithm based on the Hahnfeldt model [15]. Impulsive control based on the Hahnfeldt model and its Carleman discretisation is carried out in [16]. Impulsive control of chemotherapy based on a predator-prey model is elaborated in [17].

We modify the algorithm described in [14] to tailor it to a tumor growth model that can describe dead tumor volume dynamics and pharmacodynamics of the drug [18], which is validated by mice experiments with chemotherapy, using pegylated liposomal doxorubicin (PLD) as cytotoxic agent [1]. The tumor growth model describes the dynamics of the living and dead tumor cells, and the drug level. In the experiments, the measured values are the sum of the living and dead tumor cells, which are considered as the output of the system. The pharmacodynamics of the drug is considered with a Hill function, and we use mixed-order pharmacokinetics to describe drug depletion. The differential equations of the model are discussed in Section II.

The modified search algorithm that provides the therapy is introduced in Section III. Due to the dead tumor volume dynamics, the sum of the living and dead tumor volumes increases initially when the therapy is started, thus an exponential decay can not be followed. Moreover, the input saturation caused by the pharmacodynamics further constrains the class of attainable trajectories, thus we generate the desired trajectory only one step ahead based on the model and the actual states as initial conditions. The desired output of the system for the next step is the achievable lowest volume, and the search algorithm looks for the input that is required to get close to this value. The distance of the achieved and desired volume is characterized by a tuning parameter, which determines the order of magnitude of the dosages and the evolution of the desired trajectory as well.

Application of the search algorithm on the tumor model is demonstrated in Section IV. The results show that the

algorithm performs well on the tumor model, and we can get much lower doses than the protocol. However, these results are only valid if the model is valid, and the parameters in the model are accurate.

II. Model

The differential equations defining the system dynamics are given by

$$\dot{x}_1 = (a-n)\,x_1 - b\frac{x_1 x_3}{ED_{50}+x_3} \tag{1}$$

$$\dot{x}_2 = nx_1 + b\frac{x_1 x_3}{ED_{50}+x_3} - wx_2 \tag{2}$$

$$\dot{x}_3 = -c\frac{x_3}{K_B+x_3} - b_k\frac{x_1 x_3}{ED_{50}+x_3} + u, \tag{3}$$

where x_1 is the time function of the living tumor volume [mm^3], x_2 is the time function of the dead tumor volume [mm^3], x_3 is the time function of the drug level [mg/kg], while u is the time function of the injection rate [mg/(kg·day)]. The differential equations define the dynamics of the underlying physiological phenomena [18], [19], i.e., tumor proliferation is described by the term ax_1 in (1) with tumor growth rate a [1/day]; (drug-independent) tumor necrosis is described by the terms $-nx_1$ in (1) and nx_1 in (2) with necrotic rate n [1/day]; the effect of the drug is considered with the term $-bx_1x_3/(ED_{50}+x_3)$ in (1), $+bx_1x_3/(ED_{50}+x_3)$ in (2) and $-b_\kappa x_1x_3/(ED_{50}+x_3)$ in (3) with drug efficacy rate b [1/day], effective median dose ED_{50} [mg/kg], and modified drug efficacy rate b_κ [mg/(kg·day·mm^3)]; the mixed-order pharmacokinetics of the drug is considered with the term $-cx_3/(K_B+x_3)$ in (3) with clearance rate c [1/day] and Michaelis-Menten konstant K_B [mg/kg]; while the washout of the dead tumor cells is described by the term $-wx_2$ in (2) with washout rate w [1/day].

The output of the system (the measured tumor volume) is the sum of the living and dead tumor volumes, i.e.,

$$y = x_1 + x_2 \tag{4}$$

with differential equation

$$\dot{y} = ax_1 - wx_2. \tag{5}$$

The parameters of the model have been identified based on measurement from mice experiments. Ten mice received pegylated liposomal doxorubicin (PLD) according to the protocol given in [1], the mice are identified by the labels PLD1-PLD10. The numerical data for PLD7 and PLD10 were unavailable, thus we only used data from eight mice for the identification in [18] and we use these data in Section IV as well. The parameters of the different mice acquired from the identification are shown in Table I. During the identification process, the initial values $x_2(0) = 0$ mm^3 and $x_3(0) = 0$ mg/kg were used, while $x_1(0)$ is considered as a parameter that needs to be estimated, thus it is listed in Table I along with the model parameters.

The aim of the experiments was to analyze the effect of resistance and show that PLD can overcome drug resistance. However, in the case of PLD1 one could observe significant resistance [1], [18], while moderate resistance can be observed for PLD8 and PLD9. Since the model can not describe resistance, we do not expect good results for these cases. However, For the cases PLD2-PLD6, the model can capture the dynamics effectively [18].

III. Therapy design

The binary search algorithm to create the discrete time impulsive therapy in [14] was created for the Hahnfeldt model that has some special characteristics that are different from the model described in Section II, i.e., the Hahnfedt model only describes living tumor volume dynamics, and does not model dead tumor volume dynamics, the tumor volume is strictly monotonously decreasing if the input dose is increased, the pharmacokinetics of the drug is linear, and there is no input saturation in the model [15]. These characteristics allow the application of a monotonously decreasing reference volume (which was described as an exponential function in [14]), and due to the monotonicity in the input and the lack of input saturation, a binary search algorithm can be used to find the required input dose to achieve the desired reference volume, since by increasing the input dose, the tumor volume can always be decreased (which may not be true if there is input saturation).

The model described in Section II describes the living and dead tumor volume dynamics, has mixed-order pharmacokinetics and input saturation caused by the pharmacodynamics of the drug. These characteristics imply that the search algorithm in [14] can not be used directly, due to the following problems:

- P1 At the start of the therapy (when the volume of dead tumor cells is low), the sum of the living and dead tumor volumes increases, since the living tumor cells become dead tumor cells (thus there is no net change in the sum), and the living tumor cells proliferate (thus their volume is increased), and the washout is initially slow (because the washout velocity depends on the dead tumor volume). Thus, as long as the ratio of the living and dead tumor volumes is such that (5) is positive, the output increases. For a successful therapy, one should achieve a tumor volume ratio such that (5) becomes negative as soon as possible. Thus, strictly monotonously decreasing reference tumor volume can not be used.
- P2 The model contains input saturation, thus there is a lower limit in the achievable tumor volumes, thus by increasing the input dose, the output can not be further decreased. This excludes the direct use of a binary search algorithm.

The therapy design is carried out using Algorithm 1 at each discrete time instant (at each investigation). Let the time between the investigations be T_s (the sampling time, measured in days), and denote the value of the states and the injection

TABLE I
THE IDENTIFIED PARAMETERS FOR THE MODEL [18] BASED ON THE MICE EXPERIMENTS [1]

Parameter	PLD1	PLD2	PLD3	PLD4	PLD5	PLD6	PLD8	PLD9
a [1/day]	0.33251014	0.30727096	0.30659619	0.30984098	0.28777381	0.29874356	0.30784321	0.31092964
b [1/day]	0.11613599	0.16921924	0.19814684	0.1798533	0.1634586	0.18360699	0.17379563	0.16690942
b_κ [mg/(kg·day·mm^3)]	0.000000615	0.000000605	0.000000602	0.00000061	0.000000619	0.000000616	0.000000617	0.000000611
c [1/day]	0.23542154	0.29746975	0.30389129	0.27168118	0.31242166	0.36544031	0.18651212	0.16078102
ED_{50} [mg/kg]	0.0000889	0.0000903	0.000104287	0.000133009	0.0000864	0.0000791	0.0000779	0.0000894
K_B [mg/kg]	0.36661411	0.36073687	0.34188486	0.22958564	0.36201885	0.37417739	0.51541433	0.40024977
n [1/day]	0.1152974	0.14752398	0.15274208	0.17321153	0.13435788	0.16124057	0.13288544	0.14492042
w [1/day]	0.34557407	0.34392401	0.33110052	0.34131477	0.34069415	0.33937546	0.33605275	0.34242884
$x_1(0)$ [mm^3]	0.011772001	6.105563	147.57776	51.473444	3.8661982	50.751527	11.022992	2.6868058

at the kth investigation (i.e., at time instant kT_s) by

$$x_1[k] := x_1(kT_s) \tag{6}$$
$$x_2[k] := x_2(kT_s) \tag{7}$$
$$x_3[k] := x_3(kT_s) \tag{8}$$
$$u[k] := u(kT_s), \tag{9}$$

with the input at the kth investigation being $u(kT_s)\delta(kT_s)$, i.e., it is not a function, but a Dirac-delta distribution, and can be interpreted such that x_3 is modified by the value $u(kT_s) = u[k]$ at time instant kT_s, thus the dimension of $u[k]$ is mg/kg, and refers to the dose of injection, not the injection rate.

The modified algorithm is shown in Algorithm 1. The first step of the modified algorithm solves problem P1 by calculating the lowest achievable output (sum of living and dead tumor volumes) for the next step, by applying large dose of input (ideally the dose tends to infinity), and calculating the tumor volumes $x_1[k+1]$ and $x_2[k+1]$ for the next time instant by solving the differential equations (1)-(3) with initial conditions $x_1[k], x_2[k]$ and $x_3[k] := x_3[k] + u[k]$ ideally with

$$\lim u[k] \to \infty. \tag{10}$$

For practical reasons, the algorithm uses $u[k] = U_{MAX}$ instead of (10), where U_{MAX} should be chosen such that it is larger than the maximal tolerable dose of the applied drug. The sum of the calculated tumor volumes $y_{ref}[k+1] = x_1[k+1] + x_2[k+1]$ will be used as the reference volume by the search algorithm. This step is carried out before the while cycle in Algorithm 1.

The required drug dose $u[k]$ to reach $y_{ref}[k+1]$ from the initial conditions $x_1[k]$, $x_2[k]$ and $x_3[k] + u[k]$ is calculated by a binary search algorithm, by specifying the search space as the interval $[u_{min}, u_{max}]$ and shrinking the interval until $u_{max} - u_{min} < TOL$, where TOL is a design parameter. In the first step, the input is the center of the interval, i.e., $u[k] = (u_{max} + u_{min})/2$. In the original algorithm in [14], if the solution is less than the desired volume, then the dose is large, thus let $u_{max} = u[k]$, otherwise let $u_{min} = u[k]$, and repeat the process until the width of the interval becomes less than the specified limit. However, this can not be applied here due to problem P2, so the algorithm is modified such that we compare the distance from the desired value to a specified limit, and if the distance of the resulting output is larger than a limit specified by the parameter ϵ as

$$y[k+1] - y_{ref}[k+1] > \epsilon y_{ref}[k+1], \tag{11}$$

then the input is too low, thus we modify the lower limit of the interval as $u_{min} := u[k]$, otherwise we modify the upper limit of the interval to $u_{max} := u[k]$. In (11) we have used the consideration that $y[k+1] \geq y_{ref}[k+1]$, thus taking the absolute value of the difference to get a distance is not required. The value of the parameter ϵ characterizes how close we get to the minimal achievable volumes, and as the results will show in Section IV, it has significant effect on the doses and the achieved trajectories as well.

IV. RESULTS

The results are verified using in silico tests shown in Figs. 1-7. The figures show the simulated tumor volumes (upper figure, green curve, where the simulated tumor volume refers to the sum of the simulated living and dead tumor volumes), the reference (desired) tumor volumes (upper figure, red x in Figs. 2-4), the injections (lower figure, green dots) and the drug levels (lower figure, blue curve). The algorithm defined in Section III is used to generate the injections for 180 days with $T_s = 6$ days for the case PLD6, and tested for all the other cases without feedback.

Figure 1 shows the simulated tumor volume and the simulated drug level if the same injections are applied to the model as in the experiments [1] for PLD6, i.e., by applying the injections according to the protocol, with initial condition $x_1(0)$ from Table I, $x_2(0) = 0$ mm^3 and $x_3(0) = 0$ mg/kg. Note that the tumor volumes are simulated, thus are not the same as in the experiments, which can be found in [1]. The applied dose was the maximal tolerable dose, i.e., 8 mg/kg, and the total amount of drug used during the therapy was 40 mg/kg.

Figures 2-4 show the in silico results of the therapy generated by Algorithm 1 with different ϵ parameter values. The value of the TOL parameter was set to $U_{MAX}/1000$, where U_{MAX} is the initial upper limit for the injection, which was set to $U_{MAX} = 10$ mg/kg for all the cases (which is over the maximum tolerable dose for PLD, which is 8 mg/kg). The initial living tumor volume was the identified value that can be found in Table I, while the initial dead tumor volume was

Data: The initial values $x_1[k]$, $x_2[k]$ and $x_3[k]$. The maximal drug injection U_{MAX} and the accuracy parameter ϵ and TOL.

Result: The minimal drug dosage $u[k]$ that is required to reach the tumor volume in the vicinity of the desired tumor volume (parameterized by ϵ) in the next step.

Let $u_{\max} = U_{MAX}$ and $u_{\min} = 0$;

Let $u = U_{MAX}$. Calculate the tumor volumes in the next time instant $(k+1)T_s$ by solving the initial value problem on time interval $[kT_s, (k+1)T_s]$ defined by (1)–(3) with initial values $x_1[k]$, $x_2[k]$, $x_3[k] + u$, denote them by $x_1[k+1]$ and $x_2[k+1]$, and let the desired tumor volume in the next time instant be $y_{ref}[k+1] := x_1[k+1] + x_2[k+1]$.

while $u_{\max} - u_{\min} > TOL$ **do**

  $u = (u_{\max} - u_{\min})/2$;

  Calculate the tumor volumes in the next time instant $(k+1)T_s$ by solving the initial value problem on time interval $[kT_s, (k+1)T_s]$ defined by (1)–(3) with initial values $x_1[k]$, $x_2[k]$, $x_3[k] + u$, denote them by $x_1[k+1]$ and $x_2[k+1]$.;

  Let $y[k+1] = x_1[k+1] + x_2[k+1]$;

  if $y[k+1] - y_{ref}[k+1] > \epsilon y_{ref}[k+1]$ **then**

    $u_{\min} := u$;

  else

    $u_{\max} := u$;

  end

end

Algorithm 1: The search algorithm to find the minimal drug delivery for the next step

set to $x_2(0) = 0$ mm^3 and the initial drug level was $x_3(0) = 0$ mg/kg for all the cases.

Figure 2 shows the case when $\epsilon = 10^{-5}$, i.e., the solution is very close to the achievable minimum (the solution is in 0.001% distance from the achievable minimum). The upper figure shows that the generated series of injections (shown by the green dots in the lower figure) define a therapy that meets the goals, i.e., the tumor volumes are coincident with the desired tumor volumes at each investigation. The maximal dose that has to be injected is 3.11 mg/kg, but it is only applied in the first treatment, from the third treatment the dose reaches the value 1.88 mg/kg and remains constant during the therapy. The total amount of drug used in the therapy is 58 mg/kg, which is larger than the amount used according to the protocol in the experiments.

Figure 3 shows the results with $\epsilon = 10^{-2}$, i.e., the distance from the reference can be larger than the previous case (the achieved tumor volume is in 1% distance from the reference). This distance can not be visually noticed from Fig. 3 on the tumor volume trajectories, which look identical to the tumor volumes in Fig. 2, however, the required doses are much lower in this case. The maximal injection dose is 0.1025 mg/kg, which is only used in the first treatment, for the remaining treatments, the injections have the same value, which is 0.0928 mg/kg. The total amount of used drug is 2.793 mg/kg, which is much smaller than the amount used in the experiments.

Figure 4 shows the results with $\epsilon = 0.1$, i.e, the distance from the desired tumor volume can be large (10%). This distance can be observed in Fig. 4, and has significant effect on the first step of the algorithm, thus on the achievable minimal tumor volume. This large distance from the reference can not ensure that the balance of the living and dead tumor volume is such that (5) is negative for most of the time, thus the therapy is not successful, and the result looks like a cycle: there are intervals where the tumor volume increases, followed by intervals where the volume decreases. The required doses are lower in this case (with minimum value of 0.0049 mg/kg, maximum value of 0.0146 mg/kg, and total drug usage 0.332 mg/kg). However, as Fig. 4 shows, the therapy is not efficient, thus we need to use smaller ϵ.

The mixed-order pharmacokinetics can be observed on the simulation results: for large doses (larger than the parameter K_B), the pharmacokinetics described by the first term in the right-hand side of (3) is close to zero order, and since the solution of a zero order (constant) differential equation is linear, the drug depletes linearly as it is shown in Figs. 1 and 2. This also implies that the second term in the right-hand side of (3) with b_κ rate has negligible effect on the drug level dynamics if the tumor volume is small (which is also indicated by the small value of b_κ, which can be observed from Table I). For smaller doses (smaller than the parameter K_B), the first term in the right-hand side of (3) is close to linear, and since the solution to a linear differential equation is exponential, we can observe exponential depletion in Figs. 3 and 4. The effect of the second term in the right-hand side of (3) is negligible as well since the tumor volumes are small.

Since the therapy generated with parameters $\epsilon = 10^{-5}$ and $\epsilon = 10^{-2}$ have similar performance, but the latter uses much lower amount of drug, we chose the therapy generated with $\epsilon = 10^{-2}$ as optimal therapy shown in Fig. 3 and tested the series of injections on the other virtual patients from Table I. We have carried out tests separately with the groups PLD2-PL6, the group PLD8-PLD9 and with PLD1.

The simulation results of the open-loop application of the therapy from Fig. 3 on the virtual patients PLD2-PLD6 are in Fig. 5. The figure shows that the therapy is successful for all the cases, the tumor shrinks to a small volume till the end of the treatment, while the drug levels are similar in all the cases.

Application of the therapy in Fig. 3 to the cases PLD8-PLD9 results in the volumes and drug levels shown in Fig. 6. For the case PLD8, the tumor volume increases (but linearly, and not exponentially), while for PLD9, the tumor volume is constant. The drug levels are different from the previous results, probably due to lower parameter c and larger parameter K_B (Table I). Since the model is not realistic for these cases, the results are not reliable.

Finally, Fig. 7 shows the in silico test carried out with the case PLD1 using the injections from the therapy in Fig. 3. The

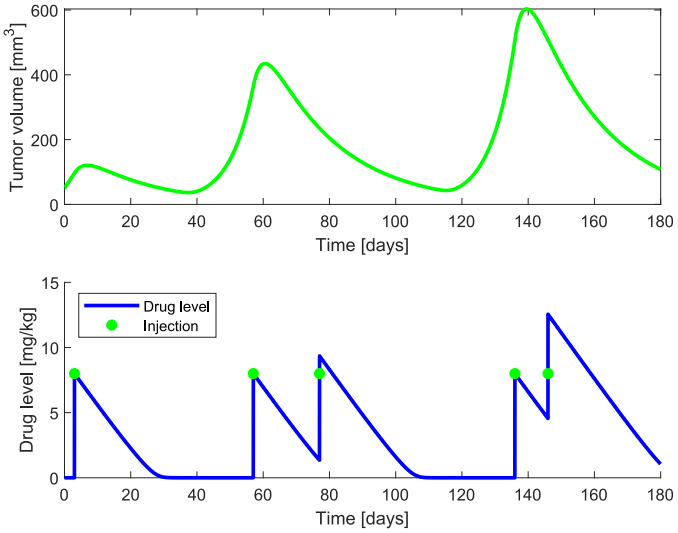

Fig. 1. The simulated tumor volume (green curve) and the injections (green dots) given according to the protocol for PLD6 in the experiments in [1], and the drug levels (blue curves).

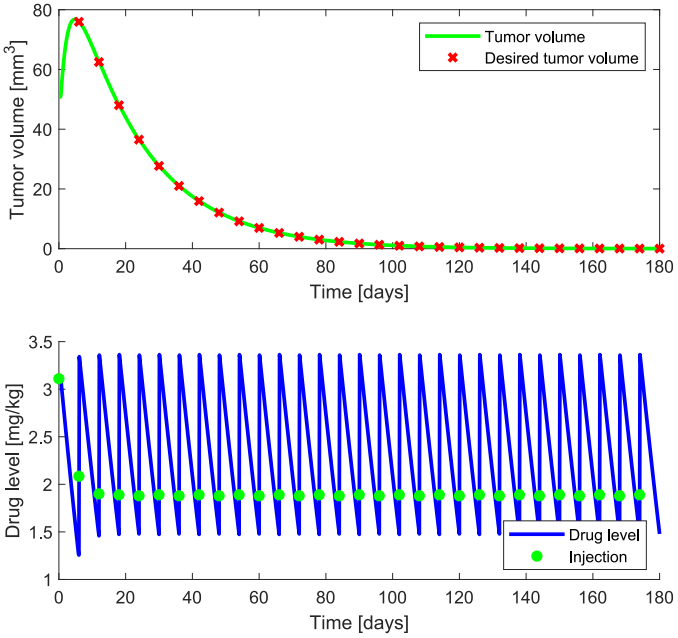

Fig. 2. The simulated tumor volume (green curve) with the desired tumor volumes (red x-s) and the injections (green dots) and the drug levels (blue curves) with $\epsilon = 10^{-5}$; the therapy is designed for PLD6.

results show that the therapy can not control tumor growth, the tumor grows exponentially. The results show that as the tumor volume reaches large values, the second-term in the right-hand side of (3) starts to dominate the dynamics of the drug (approximately after day 120), and the drug depletes fast. However, the model is not valid for this case, since the model can not describe the drug resistance, thus this result is not reliable either.

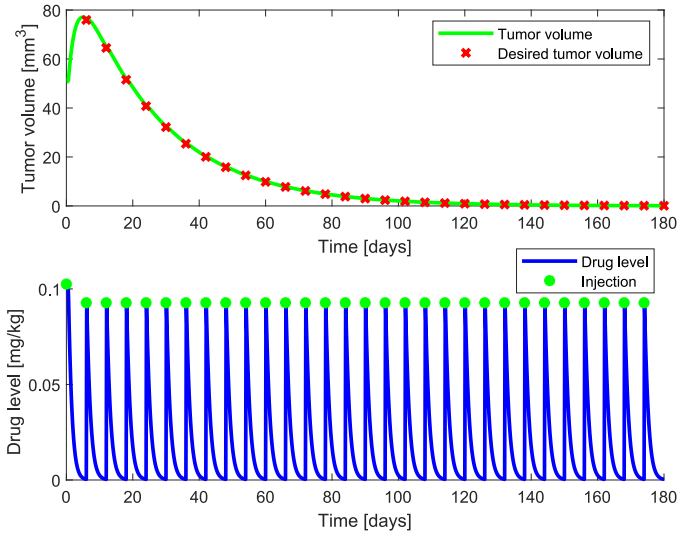

Fig. 3. The simulated tumor volume (green curve) with the desired tumor volumes (red x-s) and the injections (green dots) and the drug levels (blue curves) with $\epsilon = 10^{-2}$; the therapy is designed for PLD6.

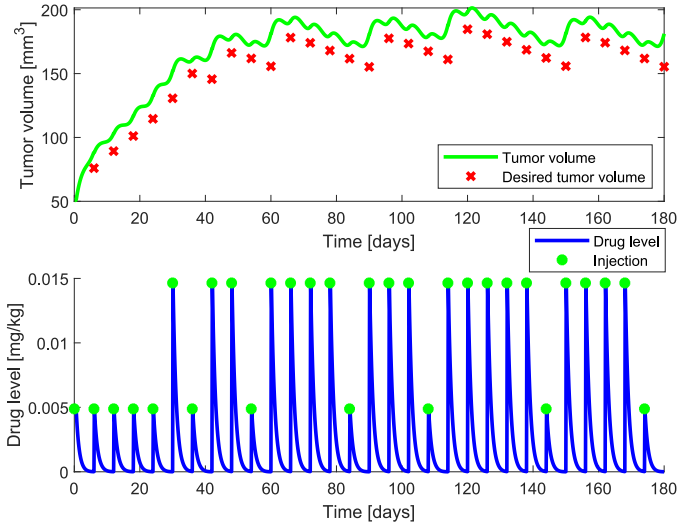

Fig. 4. The simulated tumor volume (green curve) with the desired tumor volumes (red x-s) and the injections (green dots) and the drug levels (blue curves) with $\epsilon = 10^{-1}$; the therapy is designed for PLD6.

V. Conclusions

The modified algorithm can be used to generate optimal discrete time, impulsive therapy to treat cancer with chemotherapy based on a model able to describe living and dead tumor volume dynamics, mixed-order pharmacokinetics and pharmacodynamics of the drug with input saturation. The result of the algorithm depends on the parameter which specifies the achievable distance from the reference output, the optimal value of the parameter should be set such that the tumor volume trajectory is desirable with low dosages. The optimal value of that parameter can be set by trial and error, more sophisticated solutions are subject to future research.

The algorithm was able to generate a series of injections

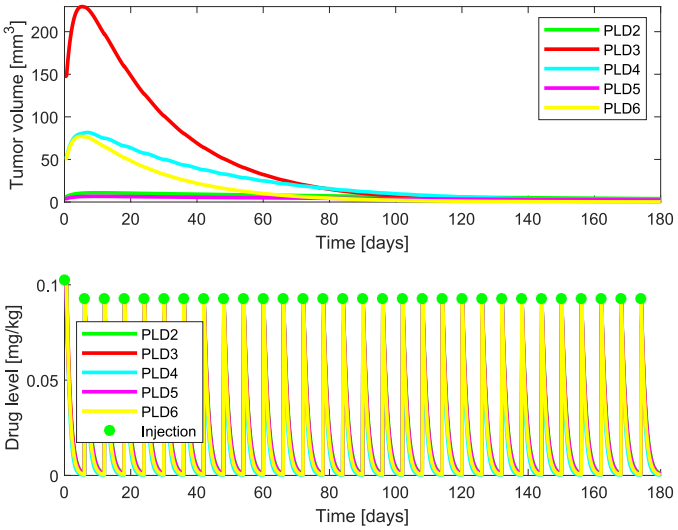

Fig. 5. The results of the application of the therapy to the virtual patients PLD2–PLD6; the simulated tumor volumes (upper figure), the injections (green dots) and the drug levels (lower figure) with the therapy designed for PLD6 with $\epsilon = 10^{-2}$.

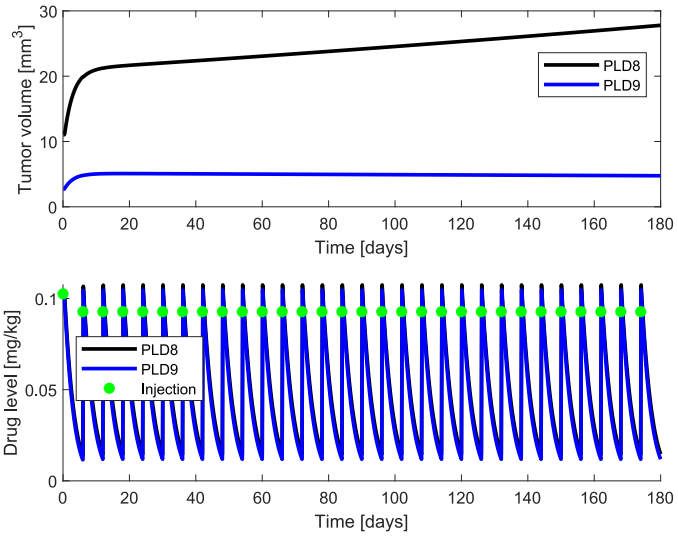

Fig. 6. The results of the application of the therapy to the virtual patients PLD8–PLD9; the simulated tumor volumes (upper figure), the injections (green dots) and the drug levels (lower figure) with the therapy designed for PLD6 with $\epsilon = 10^{-2}$.

with 6 days of sampling time which was more effective than the protocol (managed to shrink the tumor and keep it in that state), used much smaller doses (0.1 mg/kg vs 8 mg/kg) and used much less drug during the 180 days (2.793 mg/kg vs 40 mg/kg). These are promising results, however, the reliability of the results depend on the accuracy of the model and its parameters. The acquired small doses are due to the low value of the identified ED_{50} parameter. However, it is possible, that the identification process stopped in a local minimum, and the identified parameter is not valid. The practical application of the algorithm should be preceded by targeted experiments aimed to get realistic values for the critical pharmacokinetic and pharmacodynamic parameters.

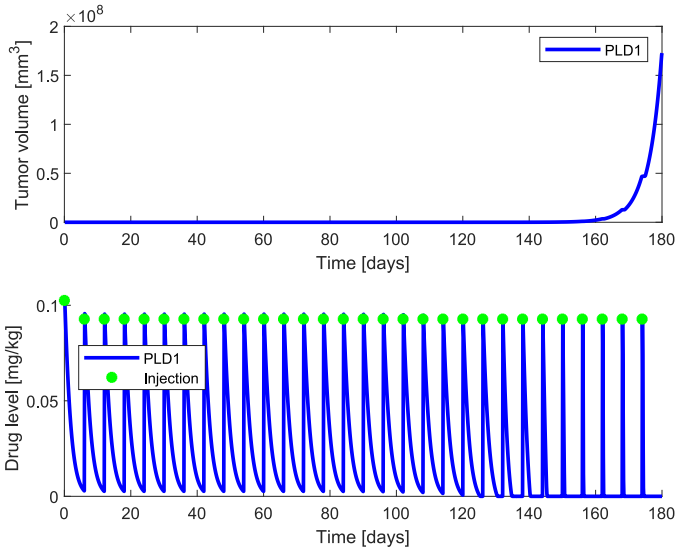

Fig. 7. The result of the application of the therapy to the virtual patient PLD1; the simulated tumor volume (upper figure), the injections (green dots) and the drug level (lower figure) with the therapy designed for PLD6 with $\epsilon = 10^{-2}$.

ACKNOWLEDGMENT

The authors would like to express their thanks to the Membrane Protein Research Group of the Hungarian Academy of Sciences for providing the measurement data. The present work has also been supported by the Hungarian National Research, Development and Innovation Office SNN 125739.

REFERENCES

[1] A. Füredi, K. Szebényi, S. Tóth, M. Cserepes, L. Hámori, V. Nagy, E. Karai, P. Vajdovich, T. Imre, P. Szabó, D. Szüts, J. Tóvári, and G. Szakács, "Pegylated liposomal formulation of doxorubicin overcomes drug resistance in a genetically engineered mouse model of breast cancer," *Journal of Controlled Release*, vol. 261, pp. 287–296, 2017.

[2] P. H. Colmegna, R. S. Sánchez-Peña, R. Gondhalekar, E. Dassau, and F. J. Doyle, "Switched lpv glucose control in type 1 diabetes," *IEEE Transactions on Biomedical Engineering*, vol. 63, no. 6, pp. 1192–1200, June 2016.

[3] P. Colmegna, F. Garelli, H. D. Battista, and R. Sánchez-Peña, "Automatic regulatory control in type 1 diabetes without carbohydrate counting," *Control Engineering Practice*, vol. 74, pp. 22 – 32, 2018.

[4] R. Gondhalekar, E. Dassau, and F. J. Doyle, "Velocity-weighting & velocity-penalty mpc of an artificial pancreas: Improved safety & performance," *Automatica*, vol. 91, pp. 105 – 117, 2018.

[5] D. Shi, E. Dassau, and F. J. Doyle III, "Multivariate learning framework for long-term adaptation in the artificial pancreas," *Bioengineering & Translational Medicine*, vol. 0, no. 0, 2018.

[6] C. M. Ionescu, T. F. Mendonca, and L. Kovács, "Critically safe general anaesthesia in closed loop: Availability and challenges," *IFAC-PapersOnLine*, vol. 48, no. 20, pp. 551 – 556, 2015, 9th IFAC Symposium on Biological and Medical Systems BMS 2015.

[7] C.-M. Ionescu, "A computationally efficient hill curve adaptation strategy during continuous monitoring of dose-effect relation in anaesthesia," *Nonlinear Dynamics*, vol. 92, no. 3, pp. 843–852, 2018.

[8] M. Alamir, M. Fiacchini, I. Queinnec, S. Tarbouriech, and M. Mazerolles, "Feedback law with probabilistic certification for propofol-based control of bis during anesthesia," *International Journal of Robust and Nonlinear Control*, vol. 28, no. 18, pp. 6254–6266, 2018.

[9] D. A. Drexler, J. Sápi, and L. Kovács, "Positive nonlinear control of tumor growth using angiogenic inhibition," *IFAC-PapersOnLine*, vol. 50, no. 1, pp. 15 068 – 15 073, 2017, 20th IFAC World Congress.
[10] D. A. Drexler, J. Sápi, and L. Kovács, "Positive control of a minimal model of tumor growth with bevacizumab treatment," in *Proceedings of the 12th IEEE Conference on Industrial Electronics and Applications*, 2017, pp. 2081–2084.
[11] D. A. Drexler, I. Nagy, V. Romanovski, J. Tóth, and L. Kovács, "Qualitative analysis of a closed-loop model of tumor growth control," in *Proceedings of the 18th IEEE International Symposium on Computational Intelligence and Informatics*, 2018, pp. 329–334.
[12] F. Cacace, V. Cusimano, A. Germani, P. Palumbo, and F. Papa, "Closed-loop control of tumor growth by means of anti-angiogenic administration," *Mathematical Biosciences & Engineering*, vol. 15, no. 4, pp. 827–839, 2018. [Online]. Available: https://doi.org/10.3934/mbe.2018037
[13] L. Kovács and G. Eigner, "Tensor product model transformation based parallel distributed control of tumor growth," *Acta Polytechnica Hungarica*, vol. 15, no. 3, pp. 101–123, 2018.
[14] D. A. Drexler, J. Sápi, and L. Kovács, "Optimal discrete time control of antiangiogenic tumor therapy," *IFAC-PapersOnLine*, vol. 50, no. 1, pp. 13 504 – 13 509, 2017, 20th IFAC World Congress.
[15] P. Hahnfeldt, D. Panigrahy, J. Folkman, and L. Hlatky, "Tumor development under angiogenic signaling: A dynamical theory of tumor growth, treatment response, and postvascular dormancy," *Cancer Research*, vol. 59, pp. 4770–4775, 1999.
[16] F. Cacace, V. Cusimano, and P. Palumbo, "Optimal impulsive control with application to antiangiogenic tumor therapy," *IEEE Transactions on Control Systems Technology*, pp. 1–12, 2018.
[17] H.-P. Ren, Y. Yang, M. S. Baptista, and C. Grebogi, "Tumour chemotherapy strategy based on impulse control theory," *Philosophical Transactions Mathematical Physical & Engineering Sciences*, vol. 375, no. 2088, 2017.
[18] D. A. Drexler, T. Ferenci, A. Lovrics, and L. Kovács, "Modeling of tumor growth incorporating the effect of pegylated liposomal doxorubicin," in *Proceedings of the 2019 IEEE 23rd International Conference on Intelligent Engineering Systems*, 2019, pp. 369–374.
[19] D. A. Drexler, J. Sápi, and L. Kovács, "Modeling of tumor growth incorporating the effects of necrosis and the effect of bevacizumab," *Complexity*, pp. 1–11, 2017.